ICIC Express Letters
Part B: Applications
Volume **7**, Number **10**, October **2016**

ICIC International ©2016 ISSN 2185-2766
pp. **2161–2167**

SKIN PANEL DESIGN FOR A MORPHING MECHANISM

Qiang Zhao[1], Xijuan Guo[1] and Fengfeng Xi[2]

[1]Key Laboratory for Computer Virtual Technology and System Integration of Hebei Province
College of Information Science and Engineering
Yanshan University
No. 438, Hebei Avenue, Qinhuangdao 066004, P. R. China
xjguo@ysu.edu.cn; hmoe@vip.qq.com

[2]Department of Aerospace Engineering
Ryerson University
Toronto, Ontario, M5B 2K3, Canada

Received March 2016; accepted June 2016

Abstract. *A segmentation method is proposed to aid rigid skin panel design for an existing modular morphing wing mechanism. The method divides the surface of the modular morphing mechanism into panels through geometry discretization, and then the skin which is made up of these rigid panels will have better rigidity and it will morph more free without any gap. The method comprises three basic morphing types based on the motion of upper platform. Wherein, the mechanism side is firstly divided into a plurality of panels and each of them is approximated to flat, and then shape changes of one panel before and after morphing are analyzed. Therefore, panels can be designed as moveable and fixed patches to achieve seamless morphing. At last, computer simulation is set up to further verify the correctness of the method.*

Keywords: Morphing mechanism, Skin panel, Surface segmentation, Seamless morphing

1. **Introduction.** The traditional fixed wing aircraft allows the aircraft to fly at a range of flight conditions, but the performance on each condition is sub-optimal. Therefore, it is greatly significant to design morphing wings adapted to multiple flight conditions. Moosavian et al. [1] considered that the ability to vary the geometry of a wing to apply to different flight conditions could significantly improve the performance of an aircraft. Now, the morphing wings are grouped into three main types [2]: planform alteration (span, sweep, and chord), out-of-plane transformation (twist, dihedral/gull, and span-wise bending), and airfoil adjustment (camber and thickness). These aircraft wings covered by rigid skin are high in stability during the morphing process, but the morphing capacity is poor and the applicable flight conditions are still limited because of the interference between rigid skins. Finistauri and Xi [3] mentioned that most wing level morphing projects focused on variable sweep, dihedral, wing twist or span, but very few combined more than one of these morphing methodologies to achieve greater morphing functionality. Finistauri et al. [4] put forward a discretization method which determined the number of morphing wing modules and the respective spacing required to emulate a known wing shape and satisfy a corresponding flight requirement. Moosavian and Xi [5] used the discretization method to design a modular morphing mechanism (Figure 1(a)) which provides the wing with individual or simultaneous sweep, dihedral, twist and span morphing. Therefore, a suitable skin is required which can cover this kind of morphing mechanism with high stiffness and controllability.

The skin of a morphing aircraft is a critical component and it must be compliant in degrees of freedom that are required for actuation, to minimize the actuation loads [6]. Because the rigid skin is hard to morph, new morphing wings have been studied and

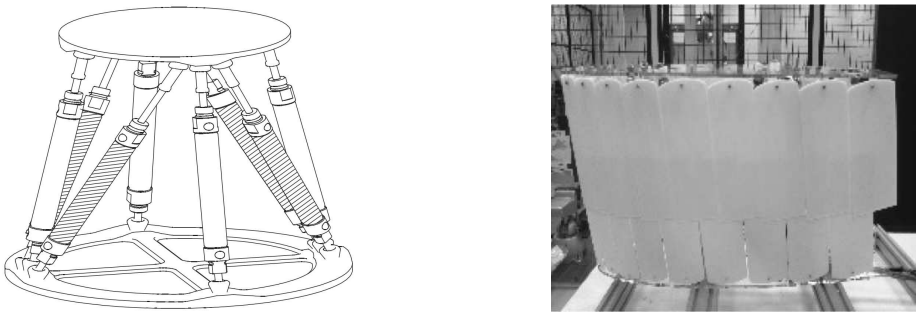

(a) The modular morphing mechanism (b) A kind of rigid morphing skin

FIGURE 1. A morphing mechanism and a kind of its rigid skin

designed, which are covered by new flexible materials and are more complex in morphing capacity to adapt to various flight conditions. Qiu et al. [7] introduced smart skins for morphing wings, and showed that smart skins designed by stiffness tailoring are good in compactness and controllability through the comparison of the wavy skin structure and the honeycomb skin structure. Murugan et al. [8] studied a variable camber morphing airfoil with compliant internal structure, flexible skin and a lightweight actuation system in a hierarchical modeling framework to improve the controllability of flexible materials. However, poor stiffness of elastic materials makes it hard to keep its shape. Rigid morphing skin is still in research. Yu et al. [9] designed a kind of rigid morphing skin with many gaps shown in Figure 1(b). The key problem is how to segment the whole surface into many movable panels and achieve the morphing result through a recombination of the panels.

Based on the modular mechanism (Figure 1(a)) in [5], a segmentation method is designed to address the segmentation problem. The method composes three steps. Firstly, the whole side of the mechanism is segmented into panels which are approximated to flat. Then three basic morphing structures are achieved to describe the whole side morphing through the motion of the upper platform when the lower platform of the mechanism is fixed. Each structure is made up of fixed patches and moveable patches through the comparison of the side before and after the upper platform movement. Finally, computer simulation graphic is given and the morphing effect is analyzed.

2. **The Morphing and Segmentation Principle.** In order to design a rigid morphed skin with the movement of the modular mechanism, the whole skin is needed to be segmented into many panels and each panel must be approximated to flat. On the premise that upper and lower platforms are circular, the side surface should be symmetric and divided into equal parts. Then the mechanism side is composed of a set of identical

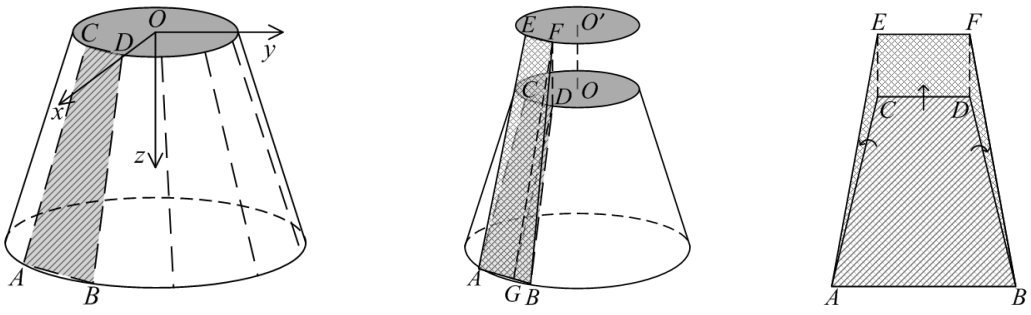

(a) (b) (c)

FIGURE 2. Schematic diagram of side segmentation and rising: (a) side segmentation, (b) upper platform rising, (c) morphing process of one panel

trapezoidal rigid panels. Once the upper platform moves, the mechanism side morphing process will be achieved based on one panel morphing process. Therefore, set the center point of the upper platform as the cartesian coordinates origin (O) and the platform in the xy-plane. The mechanism side is divided as shown in Figure 2(a) and then the three basic morphing structures are discussed.

2.1. **Upper platform rising.** When the upper platform rises, the height of the mechanism will change and the skin panels are shown in Figure 2(b). Obviously, quadrilateral $ABDC$ is not changed when side CD is moved to side EF. Therefore, $ABDC$ is designed as a fixed patch. Then moveable patches AEC, $CDFE$ and BDF are moved to form the quadrilaterals $ABDC$ and $ABFE$ (the morphing process is shown in Figure 2(c)). The moveable patches must be covered by $ABDC$. If moveable patches are too large, they should be segmented into many smaller patches. The size of the fixed patch and the moveable patches will be easily acquired after the rising distance of the upper platform and the radii of the platforms are obtained.

2.2. **Upper platform translation.** As shown in Figure 3(a), when the upper platform is moved from point O to point O', points C and D will be moved to points E' and F' and then panel ① will be morphed into panel ③. The morphing process comprises two steps. The first step is morphing panel ① into panel ②. In this process, panel ① is rotated around edge AB to coincide with surface S where panel ③ is located, and then panel ② ($ABFE$) and intersections E, F of line $E'F'$ are obtained. This morphing process is the same with that in Section 2.1.

As shown in Figure 3(a), the auxiliary line DG satisfying $DG \perp AB$ is the height of trapezoid $ABDC$. Then $FG \perp AB$ can be easily acquired after panel ① rotates along side AB and AB is perpendicular to surface DGF. Because of $AB//CD//EF$, there are $CD \perp DF$, $EF \perp DF$ and the distance d between lines CD and EF can be obtained. Set the length of CE as d, the height and side bus of mechanism be h and t respectively. After another auxiliary line GQ satisfying $GQ \perp DF$ is made in surface DGF, the rotate angle $arccos\left(\left(t^2 + l_{GF}^2 - d^2\right)/2tl_{GF}\right)$ can be achieved in which l_{GF} is the distance between lines AB and EF. This angle can also be calculated through the normal vectors of planes ① and ③.

In the second step, panel ② should be morphed into panel ③. Surface S is drawn into Figure 3(b). After an auxiliary line $E'N$ satisfying $\angle AE'N = \angle E'NB$ is made, then another auxiliary line BM satisfying $BM//E'N$ is made. Obviously, the quadrilateral $ME'NB$ is isosceles trapezoid. Make an auxiliary line $F'P$ satisfying $F'P \perp BM$ and $F'P \perp E'N$. Then $\triangle ABM$ is not changed during the morphing process and $\triangle NE'F'$ only moves with side EF; therefore, $\triangle ABM$ and $\triangle NEF$ are fixed patches.

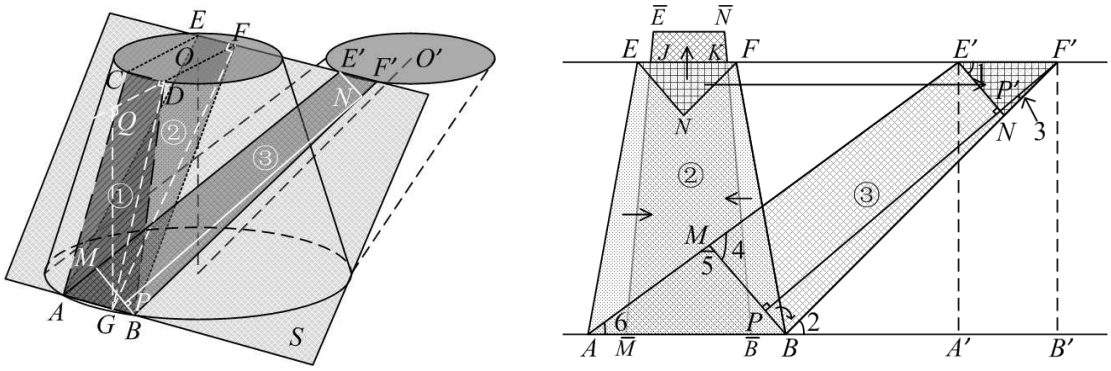

(a) Upper platform translation (b) Morphing process in surface S

FIGURE 3. Schematic diagram of translation

It can be acquired from Figure 3(b) that $\angle ABM = \angle NE'F' = \angle 1$, $\angle E'F'N = \angle F'BB' = \angle 2$, $\angle PF'B = \angle 3$, $\angle E'MB = \angle E'NF' = \angle NBM = \angle 4$, $\angle AMB = \angle AE'N = \angle E'NB = \angle 5$ and $\angle E'AB = \angle 6$. Then let the length of FF', EF, AB, $A'E'$ be l_1, l_2, l_3, l_4. According to these variables, $l_{AA'} = l_1 + (l_3 - l_2)/2$ and $l_{BB'} = l_1 - (l_3 - l_2)/2$ can be acquired. And then $\angle 2 = \arctan(l_1/l_{BB'})$ and $\angle 6 = \arctan(l_1/l_{AA'})$ are easily obtained. Because $\angle 4 = \angle 6 + \angle 1$ and $\angle 5 = \angle 1 + \angle 2$, $\angle 1 = (\pi - \angle 2 - \angle 6)/2$ is obtained, and then all the interior angles of $\triangle ABM$ and $\triangle E'F'N$ are obtained. Then, the set of fixed patches $\{(\angle 6, \angle 5, l_{AB}), (\angle 1, \angle 2, l_{E'F'})\}$ is achieved.

Then the morphing process from $ABFE$ to $BME'N$ which is the same with $\overline{BMEN}$ should be analyzed. $l_{P'P} = l_4 \sin\angle 4 / \sin\angle 2 - l_2 \sin\angle 1$ can be easily acquired from Figure 3(b). If $\angle 4 < \angle 2$ and $l_{P'P} < l_4$, $ABFE$ will be larger than $BME'N$. Therefore, the moveable patches $A\overline{M}JE$, $\overline{E}JK\overline{N}$ and $FK\overline{B}B$ should be moved under $\overline{BMEN}$. If $\angle 4 > \angle 2$ and $l_{P'P} > l_4$, $ABFE$ will be shorter than $BME'N$. As shown in Figure 3(b), the moveable patches $A\overline{M}JE$ and $FK\overline{B}B$ should be moved under $\overline{BM}JK$ and $\overline{E}JK\overline{N}$ should be stretched out. Then the morphing process is finished after $BME'N$ is rotated around point B from $\overline{BMEN}$.

2.3. **Upper platform rotation.** As shown in Figure 4(a), after the upper platform is rotated θ degree around L-axis, segment CD will be moved to segment EF. Because CD is not always parallel to EF, quadrilateral $ABFE$ is not always a plane. Therefore, $ABFE$ is needed to be divided into triangles since triangle is always a plane. The morphing process consists of two parts: $\triangle ABC$ is morphed into $\triangle ABE$ and $\triangle BCD$ into $\triangle BEF$. The former is called independent morphing process, and the latter is called dependent morphing process. In the independent process, the common side AB is unchangeable.

Set $\overrightarrow{AB} = \vec{a}$, $\overrightarrow{BC} = \vec{b}$ and $\overrightarrow{BE} = \vec{c}$. Then the normal vectors of surfaces ABC and ABE are $\left(\vec{a} \times \vec{b}\right)$ and $(\vec{a} \times \vec{c})$, whose included angle is the rotation angle $\left(\alpha = \arccos\left(\left(\vec{a} \times \vec{b}\right) \cdot (\vec{a} \times \vec{c}) \,/\, \left\|\vec{a} \times \vec{b}\right\| \cdot ||\vec{a} \times \vec{c}||\right)\right)$. After $\triangle ABC$ is rotated α degree along side AB, the coordinate of point C will be C'. $C' = C\cos\alpha + (C \cdot \vec{a})C(1 - \cos\alpha) + (C \times \vec{a}\sin\alpha)$. According to the coordinate of point C', there are three position relations between $\triangle ABC'$ and $\triangle ABE$ as respectively shown in Figure 4(b), Figure 4(c) and Figure 4(d). The fixed patches are $\triangle ABO$, $\triangle ABC'$ and $\triangle ABE$ respectively. Through the coordinates of points A, B, C' and E, the sides and interior angles of $\triangle ABE$ and $\triangle ABC'$ can be calculated. Then the moveable patches in the figures can be acquired.

In the dependent morphing process, the length of CD is always equal to that of EF and point B keeps unchangeable, but side BC will be morphed into BE based on the independent morphing process. Because segment BC is a diagonal of trapezoid $ABCD$ as shown in Figure 4(a), side BC is the longest side of $\triangle BCD$ and $\angle BDC$ is an obtuse

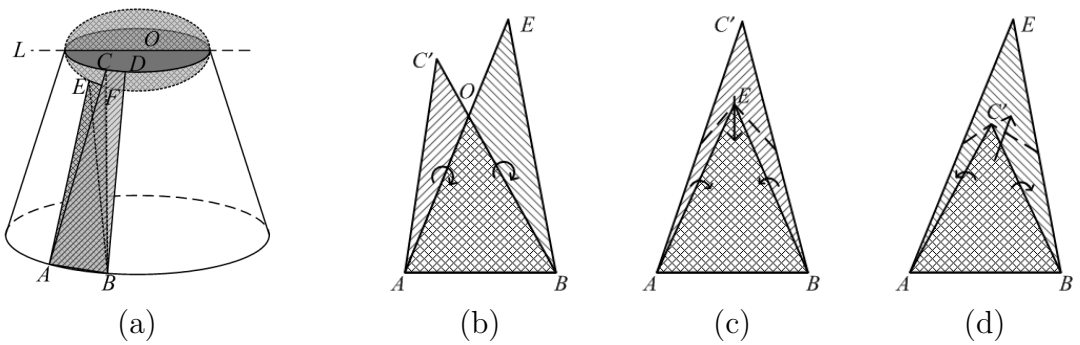

FIGURE 4. Schematic diagram of rotation and independent morphing process: (a) upper platform rotation, (b) two triangles with one intersection, (c,d) one triangle in another one

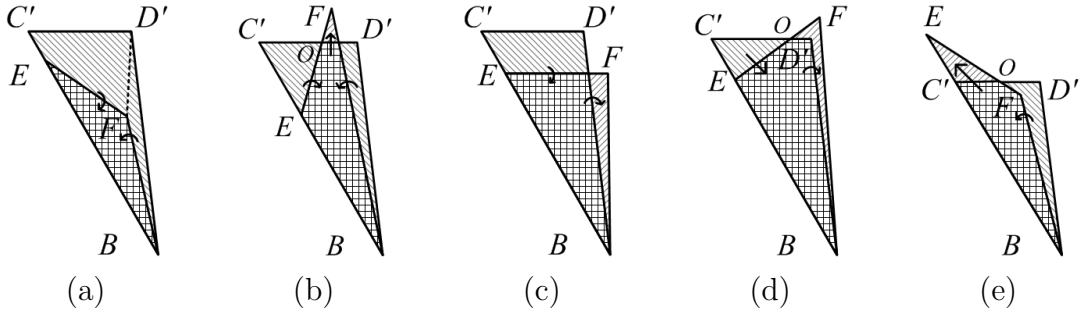

FIGURE 5. Five position relations in dependent morphing process

angle. Therefore, $\triangle BCD$ is rotated to $\triangle BC'D'$ existing on the surface of $\triangle BEF$. When lines BC' and BE coincide, five position relations will be established between $\triangle BD'C'$ and $\triangle BEF$ in Figure 5.

Therefore, a comparison method is proposed to distinguish the different position relations. The method consists of three steps: 1) comparing the length of BC' and that of BE; 2) comparing the value of $\angle C'BD'$ and that of $\angle FBE$; 3) comparing the value of $\angle BD'F$ and that of $\angle BD'C'$ when $\angle C'BD' > \angle EBF$, comparing the value of $\angle BD'F$ and that of $\angle BEF$ when $\angle C'BD' < \angle EBF$ and comparing the length of BF and that of BD' when $\angle C'BD' = \angle EBF$.

As shown in Figures 4 and 5, panel $ABDC$ is morphed into two panels $\triangle ABE$ and $\triangle EFB$ which reconstruct panel $ABFE$, which shows that the morphing process is finished.

3. **Simulation and Analysis.** According to the method proposed in Section 2, computer program is developed to prove the feasibility of the principle. In order to facilitate a comparative analysis, set the radius of upper and lower platform, the height of mechanism as 1m, 1.5m and 1m respectively. Then several simulations are given as follows based on four different values of k. k means the number of equal parts which the mechanism side is divided into. In this paper, $k = 10$, $k = 30$, $k = 60$ and $k = 100$, respectively.

3.1. **Computer simulation.** After the upper platform translations 0.5m, the mechanism side before and after morphing process will be shown in Figure 6(a), Figure 6(b), Figure

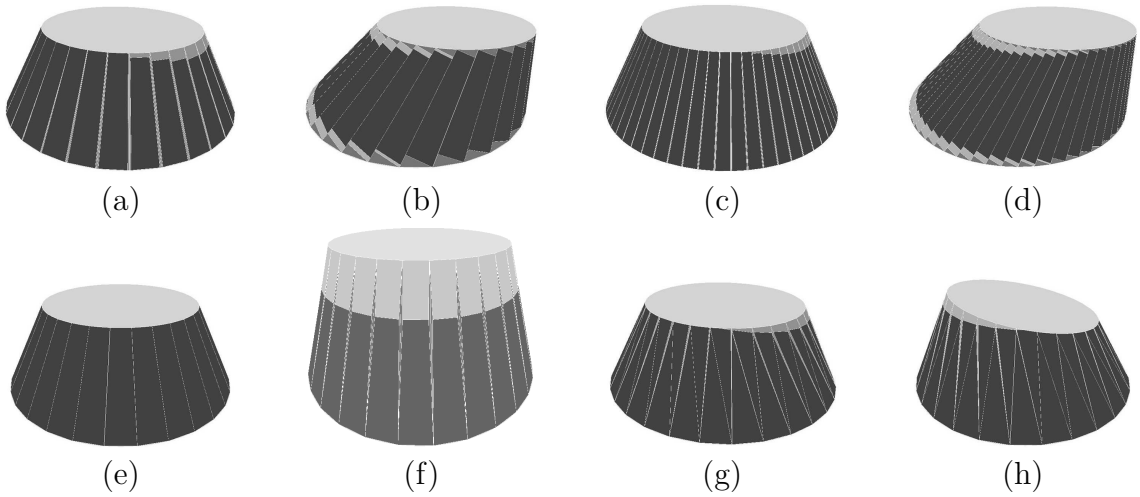

FIGURE 6. Schematic diagram of computer simulation: (a,b) translation simulation when $k = 30$, (c,d) translation simulation when $k = 60$, (e,f) rising simulation when $k = 30$, (g,h) rotation simulation when $k = 30$

6(c) and Figure 6(d). Dark grey represents the fixed patches. Light grey represents the moveable patches required to be moved during the morphing process.

As shown in Figure 6, the bigger k is, the narrower the panels are and then the smoother the side is. After the upper platform rises 0.5m along the z-axis, the mechanism side will be shown as Figure 6(e) and Figure 6(f) before and after morphing process. The mechanism side before and after the upper platform rotating 10° is shown as Figure 6(g) and Figure 6(h). The partition granularity is related to the value of k.

3.2. **Computation time analysis.** Figure 7(a) shows the relation among the translation distance of upper platform, the computation time and the value of k. According to Figure 7, it can be concluded that the computation time is only related to the value of k. The bigger k is, the longer the time is used.

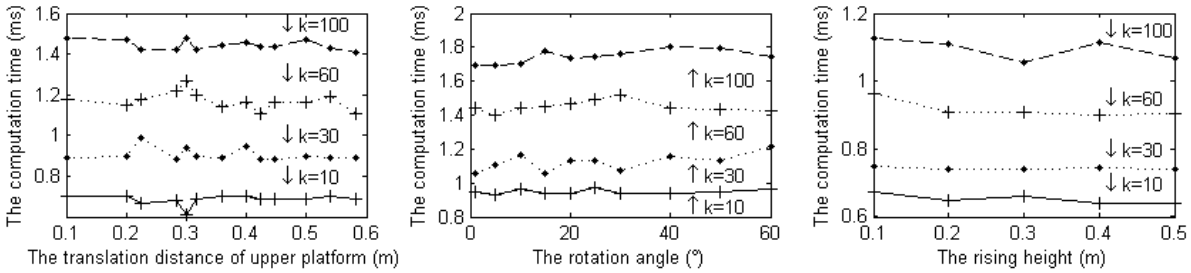

(a) (b) (c)

FIGURE 7. Computation time: (a) translation computation time, (b) rotation computation time, (c) rising computation time

Therefore, the computation time and the segmentation granularity only depend on the value of k. Figure 7 shows that the longest computation time is less than 2ms when $k = 100$.

3.3. **CAD software simulation.** Based on the above computation result, morphing panels are designed in CAD software as shown in Figure 8. Along with the movement of mechanism, the mechanism side will be morphed smoothly without any gap.

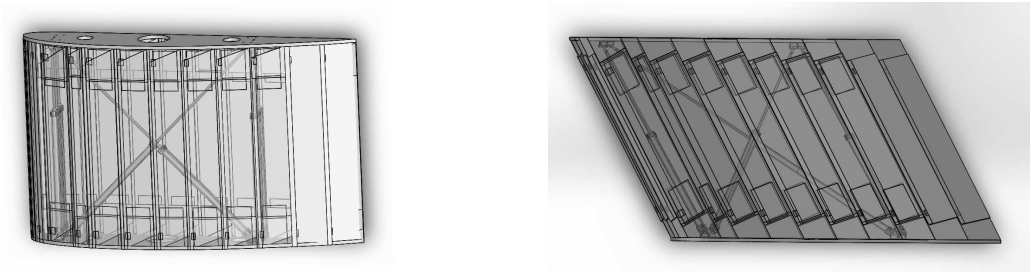

(a) (b)

FIGURE 8. Schematic diagram of CAD simulation: (a) skin panels before morphing, (b) skin panels after morphing

4. **Conclusions.** A segmentation method is proposed to aid rigid skin panel design for an existing modular morphing wing mechanism. The main research is which shape of the skin should be designed to ensure that there exists no gap during the morphing process. All the morphing panels can be constructed by the combination of three basic types. Although the segmentation result is related with the shape of platforms, the height of mechanism, the state before and after morphing and the value of k, the segmentation granularity and the computation time are only related with k. The computation is quick

enough and the CAD software simulation results prove that panels designed by the method can be morphed without any gap.

Acknowledgment. This work is supported by the Science and Technology Support of Hebei Province under Grant No. 15211019D.

REFERENCES

[1] A. Moosavian, F. Xi and S. M. Hashemi, Design and motion control of fully variable morphing wings, *AIAA Journal of Aircraft*, vol.50, no.4, pp.1189-1201, 2013.

[2] S. Barbarino, O. Bilgen, R. M. Ajaj, M. I. Friswell and D. J. Inman, A review of morphing aircraft, *Journal of Intelligent Material Systems and Structures*, vol.22, no.9, pp.823-877, 2011.

[3] A. D. Finistauri and F. Xi, Type synthesis and kinematics of a modular variable geometry truss mechanism for aircraft wing morphing, *Proc. of the ASME/IFToMM International Conference on Reconfigurable Mechanisms and Robots*, Fairfield, NJ, pp.478-485, 2009.

[4] D. Finistauri, F. Xi and P. Walsh, Discretization method for the development of a modular morphing wing, *AIAA Journal of Aircraft*, vol.49, pp.116-125, 2012.

[5] A. Moosavian and F. Xi, Design and analysis of recon gurable parallel robots with enhanced stiffness, *Mechanism and Machine Theory*, vol.77, pp.92-110, 2014.

[6] A. D. Shaw, I. Dayyani and M. I. Friswell, Optimisation of composite corrugated skins for buckling in morphing aircraft, *Composite Structures*, vol.119, pp.227-237, 2015.

[7] J. Qiu, C. Wang, C. Huang, H. Ji and Z. Xu, Smart skin and actuators for morphing structures, *Procedia IUTAM*, vol.10, pp.427-441, 2014.

[8] S. Murugan, B. K. S. Woods and M. I. Friswell, Hierarchical modeling and optimization of camber morphing airfoil, *Aerospace Science and Technology*, vol.42, pp.31-38, 2015.

[9] A. Yu, F. Xi and D. Finistauri, Kinematic modelling of a panel enclosed hexapod, *Mechanisms and Machine Science*, vol.36, pp.419-431, 2016.